Two-stage effects of awareness cascade on epidemic spreading in multiplex networks

Quantong Guo, Xin Jiang, Yanjun Lei, Meng Li, Yifang Ma, and Zhiming Zheng

Phys. Rev. E **91**, 012822 — Published 28 January 2015

DOI: 10.1103/PhysRevE.91.012822

Two-stage effects of awareness cascade on epidemic spreading in multiplex networks

Quantong Guo,[1,2] Xin Jiang,[1,2,*] Yanjun Lei,[2,3] Meng Li,[1,2] Yifang Ma,[2,3] and Zhiming Zheng[1,2,3,†]

[1]*School of Mathematics and Systems Science, Beihang University, Beijing 100191, China*
[2]*Key Laboratory of Mathematics Informatics Behavioral Semantics(LMIB), Ministry of Education, China*
[3]*School of Mathematical Sciences, Peking University, Beijing 100191, China*

Human awareness plays an important role in the spread of infectious diseases and the control of propagation patterns. The dynamic process with human awareness is called awareness cascade, during which individuals exhibit herd-like behavior because they are making decisions based on the actions of other individuals (Journal of Complex Networks (2013) 1, 3-24). In this paper, to investigate the epidemic spreading with awareness cascade, we propose a local awareness controlled contagion spreading model on multiplex networks. By theoretical analysis using a microscopic Markov chain approach and numerical simulations, we find the emergence of an abrupt transition of epidemic threshold β_c with the local awareness ratio α approximating 0.5, which induces two-stage effects on epidemic threshold and the final epidemic size. These findings indicate that the increase of α can accelerate the outbreak of epidemics. Furthermore, a simple 1D lattice model is investigated to illustrate the two-stage like sharp transition at $\alpha_c \approx 0.5$. The results can give us a better understanding of why some epidemics can not break out in reality and also provide a potential access to suppressing and controlling the awareness cascading systems.

PACS numbers: 89.65.-s, 89.75.Fb, 89.75.Hc

I. INTRODUCTION

Epidemic spreading is an important phenomenon which has been extensively studied [1–10] in the field of complex network. There have been various models which can be used to shed light on these dynamic processes, including the classical susceptible-infected-susceptible model(SIS) [11], susceptible-infected-recovery model(SIR) [12] and so on [13, 14]. These models have focused on various factors which can affect epidemic spreading, e.g., the frequency of contacts between people [15, 16], duration of the disease [17, 18], immunity of particular individuals [19], etc.

Very recently, there has been growing interest in investigating the interplay between human response and epidemic spreading [14, 20–23], especially the awareness, or risk perception which can be considered as a crucial feature in the reduction of susceptibility when individuals become aware of the epidemics. Funk *et al*. [24] found that in a well-mixed population, awareness of epidemics can lead to a lower size of the outbreak, but can not affect the epidemic threshold. Moreover, Wu *et al*. [25] classified the awareness into three categories, the so called local awareness, global awareness and contact awareness. They show that global awareness cannot decrease the likelihood of an epidemic outbreak while the other two types of awareness can decrease it.

Furthermore, as a natural way to describe the interrelated different interactions among people, multiplex network [27–32] has been gaining more and more attentions in exploring epidemic spreading with respect to awareness [23, 26]. Two interdependent networks can be used for modeling the co-evolution of disease and the awareness dynamic process. By considering the dynamic interplay between awareness and epidemic spreading in multiplex networks, Granell *et al*. [26] discovered the emergence of a metacritical point where the diffusion of awareness is able to control the onset of epidemics. A common feature of these models mentioned above is that the dynamic process of the spreading of awareness and epidemics is the same.

However, in real cases, the way awareness spreading is quite different from which epidemics do. For instance, when one occasionally reads a message about epidemics on Facebook or other social networks, he may not take actions, which means he doesn't become aware of it. But when the proportion of his friends who have been aware of the epidemics surpasses a critical point, he may take measures with high probability, in other words, one can become aware of the epidemics according to the states of its friends. This herd-like feature is just like the way we make decision to accept one idea or reject it in our daily life [33–35]. Here, we introduce a threshold model to describe this phenomenon and the threshold in the transformation process of awareness state is named as local awareness ratio in our work.

In this paper, we propose a local awareness controlled contagion spreading(LACS) model on top of multiplex networks to study the interplay between the spreading of epidemic and awareness. In the model, we find an interesting phenomenon that epidemic threshold may undergo an abrupt transition when local awareness ratio is set to be 0.5. Moreover, the final epidemic size also appears to display two distinct phases around this critical value. When local awareness ratio is smaller than 0.5, the epidemic threshold is the bigger one and the final epidemic size is almost the same. Otherwise, the final epidemic size increases significantly with the increasing of local aware-

* jiangxin@buaa.edu.cn
† zzheng@pku.edu.cn

ness ratio but the epidemic threshold is the smaller one. Analytically, we extend the microscopic Markov chain approach (MMCA) [26] to derive the epidemic threshold of our model and numerical simulations show that the MMCA has a high accuracy for the prediction of the epidemic threshold.

The rest of this paper is organized as follows: In Sec. II, we describe the LACS model and the dynamic process on it; in Sec. III, we use MMCA to analyze the epidemic threshold of our model; in Sec. IV, we present numerical simulations and compare these with theoretical results. We also investigate the effects of different local awareness ratios on the spread of epidemics, meanwhile, a 1D lattice model is proposed to investigate the two-stage effects; in Sec. V, we conclude the paper and make some discussions.

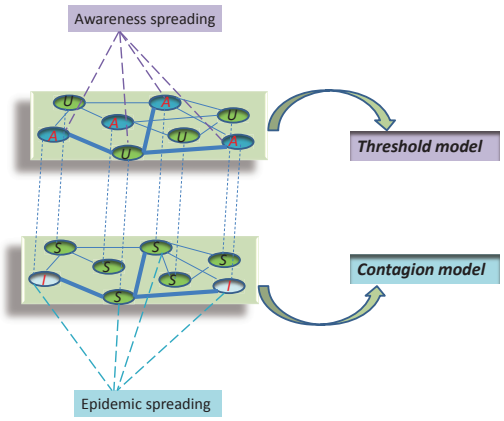

FIG. 1. (Color online) Example of the structure of multiplex network used in our work. The upper layer corresponds to the network where the spreading of awareness happens, nodes on this layer have two kinds of states: unaware and aware. The other layer represents the epidemic spreading with two kinds of states, including susceptible and infected. Only three kinds of states can exist in this multiplex network: unaware and susceptible, aware and infected, aware and susceptible. The spreading models of awareness and epidemic are different, with threshold model and contagion model for the upper and lower layer, respectively.

II. THE LOCAL AWARENESS CONTROLLED CONTAGION SPREADING MODEL

Our model is implemented on a multiplex network. To illustrate it, we construct a two-layer network, see FIG.1. The first layer represents individual's awareness of epidemics. On this layer, if one individual is aware of epidemics, its state is Aware (A), otherwise its state is Unaware (U). The second layer corresponds to individual's physical states of epidemics, which means if an individual is infected, its state is Infected (I), else its state is Susceptible (S). For the sake of simplicity, we assume this multiplex network is unweighted and undirected. The interconnection between two layers is responsible for the coupled dynamic process of the spreading of epidemics and awareness.

As mentioned above, individuals on the awareness layer spread the awareness of epidemics while contagion process takes place on the contagion layer. The evolution of the awareness dynamic process is defined as follows: on the one hand, unaware individuals become aware due to two reasons: the radio between their aware neighbors and their degrees, number of links connected with them, reaches the critical value (local awareness ratio α) or unaware individuals is already infected. On the other hand, aware individuals change into the state of unaware in two ways: the individual is susceptible again or have forgotten the awareness (with a probability δ).

Similar to the classical epidemic model (SIS), on the contagion layer, a susceptible individual can be infected by an infectious neighbor with probability β while infected ones can recover to be susceptible with probability μ at the same time. If an individual is infected, it is naturally that this individual becomes aware of the epidemic. However, the infectivity β can be reduced by a factor if one is aware of the epidemic. We use β^U and β^A to represent the infection rates without and with awareness, respectively. For the sake of simplicity, here we assume $\beta^A = 0$, which corresponds to complete immunity of individuals aware of the epidemic. It is worth noting that each individual in this multiplex network can only have three kinds of states: unaware and susceptible (US), aware and infected (AI), aware and susceptible (AS).

III. THE MMCA METHOD ON THE LACS MODEL

In this section, to illustrate the use of MMCA method[36, 37] which is a discrete-time version of the evolution of epidemics by means of Markov chain, we introduce the probability tree method. In FIG. 2, we reveal the possible states and their transitions in the LACS model, just as defined in[26]. Here, let a_{ij}, b_{ij} be the adjacency matrices of the awareness layer and the contagion layer, respectively. Since individual i has to be one of the three states at time t, we denote the probabilities as $p_i^{AI}(t)$, $p_i^{AS}(t)$, $p_i^{US}(t)$, respectively. Then on the awareness layer, we define the probability for unaware individual i not changing from state U to state A as $r_i(t)$; on the contagion layer, we define the probabilities for individual i not being infected by any neighbors if i was aware as $q_i^A(t)$, and not being infected by any neighbors if i was unaware as $q_i^U(t)$.

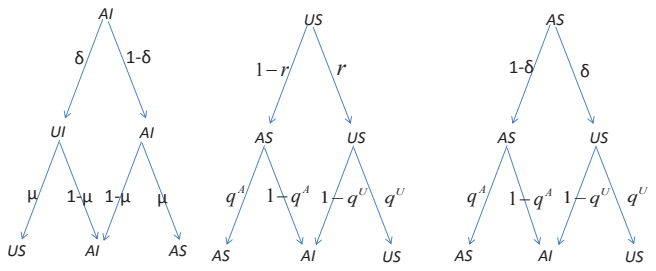

FIG. 2. Transition probability trees for the states. The states include AI (aware and infected), US (unaware and susceptible), AS (aware and susceptible). Note that μ represents transition probability from infected to susceptible, δ represents transition probability from aware to unaware, q^A represents transition probability for individual not being infected by neighbors if it is aware, q^U represents transition probability for individual not being infected by neighbors if it is unaware, r represents probability for individual not changing from unaware to aware. The coupled dynamic process takes place consecutive as time goes by.

With respect to the above definitions, we have

$$\begin{aligned} r_i(t) &= \mathbf{H}(\alpha - \frac{\sum_j a_{ji} p_j^A(t)}{k_i}) \\ q_i^A(t) &= \prod (1 - b_{ji} p_j^{AI}(t) \beta^A) \\ q_i^U(t) &= \prod (1 - b_{ji} p_j^{AI}(t) \beta^U) \end{aligned} \tag{1}$$

Note that Eqs.(1) are obtained supposing independence on the contribution from the neighbors, which is the only approximation in MMCA[23, 26]. $\mathbf{H}(x)$ is a Heaviside step function, i.e., if $x > 0$, $\mathbf{H}(x) = 1$, else $\mathbf{H}(x) = 0$. In other words, $r_i(t)$ can only be 0, when the fraction of its aware neighbors surpasses local awareness ratio α, or 1 if the fraction of its aware neighbors is less than local awareness ratio α.

Then, the evolution equations of three different states can be described as follows by using the MMCA method[26]:

$$\begin{aligned} &p_i^{US}(t+1) = p_i^{AI}(t)\delta\mu + p_i^{US}(t) r_i(t) q_i^U(t) + p_i^{AS}\delta q_i^U(t) \\ &p_i^{AS}(t+1) = p_i^{AI}(t)\mu(1-\delta) + p_i^{US}[1 - r_i(t)] q_i^A(t) \\ &+ p_i^{AS}(1-\delta) q_i^A(t) \\ &p_i^{AI}(t+1) = p_i^{AI}(t)(1-\mu) + p_i^{US}(t)\{[1 - r_i(t)][1 - q_i^A(t)] \\ &+ r_i(t)[1 - q_i^U(t)]\} + p_i^{AS}(t)\{\delta[1 - q_i^U(t)] \\ &+ (1-\delta)[1 - q_i^A(t)]\} \end{aligned} \tag{2}$$

There exists an epidemic threshold β_c for the coupled dynamic process. The epidemic threshold indicates that for infection strengths β below the epidemic threshold β_c, initial epidemics quickly die out. While for infection strengths β above the epidemic threshold β_c, the epidemics can outbreak in the population. We use the stationary solution of the system of Eqs.(2) to get β_c by letting $t \to \infty$, which means $p_i^{AI}(t+1)_{t\to\infty} = p_i^{AI}(t)_{t\to\infty} = p_i^{AI}$, $p_i^{AS}(t+1)_{t\to\infty} = p_i^{AS}(t)_{t\to\infty} = p_i^{AS}$, $p_i^{US}(t+1)_{t\to\infty} = p_i^{US}(t)_{t\to\infty} = p_i^{US}$. Near the epidemic threshold, the probability for nodes being infected can be assumed as $p_i^{AI} = \epsilon_i \ll 1$. Then, the probabilities for individuals not being infected by neighbors are described as follows according to the above assumption.

$$\begin{aligned} q_i^A &= \prod (1 - b_{ji} p_j^{AI} \beta^A) \\ &\approx (1 - \beta^A \Sigma_j b_{ji} \epsilon_j) \end{aligned} \tag{3}$$

$$\begin{aligned} q_i^U &= \prod (1 - b_{ji} p_j^{AI} \beta^U) \\ &\approx (1 - \beta^U \Sigma_j b_{ji} \epsilon_j) \end{aligned} \tag{4}$$

Considering the stationary probabilities of three different states p_i^{US}, p_i^{AS}, p_i^{AI} with respect to Eq.(3) and Eq.(4), we obtain the reduced stationary equations upon omitting higher order items:

$$p_i^{US} = p_i^{US} r_i + p_i^{AS} \delta \tag{5}$$

$$p_i^{AS} = p_i^{US}(1 - r_i) + p_i^{AS}(1 - \delta) \tag{6}$$

Furthermore, we get the probability for node i being infected ϵ_i

$$\begin{aligned} \mu\epsilon_i &= p_i^{US}((1 - r_i)\beta^A \Sigma_j b_{ji} \epsilon_j + r_i \beta^U \Sigma_j b_{ji} \epsilon_j) \\ &+ p_i^{AS}(\delta\beta^U \Sigma_j b_{ji} \epsilon_j + (1-\delta)\beta^A \Sigma_j b_{ji} \epsilon_j) \\ &= (p_i^{AS}\beta^A + p_i^{US}\beta^U) \Sigma_j b_{ji} \epsilon_j \end{aligned} \tag{7}$$

It's clear that $p_i^{AI} + p_i^{AS} + p_i^{US} = 1$, where $p_i^A = p_i^{AI} + p_i^{AS}$. Noting that $p_i^{AI} = \epsilon_i \ll 1$, we get $p_i^{AI} \approx p_i^A$ and $p_i^{US} = 1 - p_i^{AI} - p_i^{AS} = 1 - p_i^A$. So Eqs.(7) can be described as

$$\mu\epsilon_i = \beta^U (1 - p_i^A) \Sigma_j b_{ji} \epsilon_j \tag{8}$$

therefore, Eqs.(8) is reduced to $\Sigma_j[(1 - p_i^A) b_{ji} - \frac{\mu}{\beta^U} t_{ji}]\epsilon_j = 0$, where t_{ji} are the elements of the identify matrix.

As a self-consistent equation, the epidemic threshold β_c reduces to the solution of eigenvalue problem. The outbreak of epidemic is the minimum value β^U satisfying Eqs.(8). Let Λ_{max} be the maximal eigenvalue of S whose elements are $s_{ji} = (1 - p_i^A) b_{ji}$. Then the critical point is written as [26]

$$\beta_c^U = \frac{\mu}{\Lambda_{max}} \tag{9}$$

IV. SIMULATIONS OF THE EPIDEMIC THRESHOLD

In Sec. III, we analytically obtain the condition for the outbreak of epidemic. Simulations of this coupled dynamic process are performed using different networks in this section to crosscheck our analytical results. In

the following, see FIG. 3, we show the comparison of Monte Carlo simulations with our theoretical predictions of epidemic threshold β_c^U.

We consider a two-layer SF network, of which the topology structures of the two layers are the same. Besides, the initial condition is set to be that 10% of nodes are infected. Iterate the rules of the coupled dynamic process with parallel updating until convergence to a steady state. The process is totally evolved for 1000 time steps. In order to reduce the fluctuation of the percent of nodes to be infected, we make time average that satisfies $\rho^I = \frac{1}{T}\Sigma_{t=t_0}^{t=t_0+T-1}\rho^I(t)$ and take T=20 (that is, $t_0 = 981$).

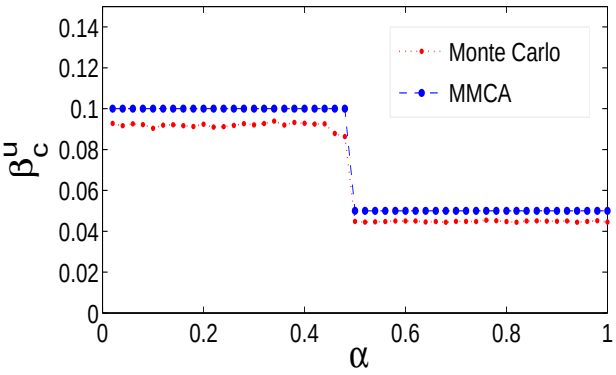

FIG. 3. (Color online) The comparison of epidemic thresholds β_c^U using the MMCA approach (blue (upper) line) and Monte Carlo simulations (red line) as a function of local awareness ratio α with a fixed value of $\delta = 0.8$. The recovery probability μ is set to 0.6. The two layers of the multiplex network are the same SF network generated by the configuration model with exponent 3. Each layer has 10^4 nodes and the average degree $\langle k\rangle = 6$. The Monte Carlo simulations is averaged by 30 realizations.

As can be seen from FIG. 3, we find good agreement between the MMCA method and simulations in calculating the epidemic threshold β_c^U and the discrepancy between MMCA and Monte Carlo can also be shown in our simulations. The reason why the analytic results always overestimate the Monte Carlo is that we suppose independence on the contribution from the neighbors in MMCA[23, 26]. Due to the assumption, the value of $r_i(t)$ in MMCA is somehow smaller than that in Monte Carlo simulations. Therefore, it is easier for the outbreak of epidemics in Monte Carlo simulations. Furthermore, we find that the epidemic threshold has an abrupt transition when the local awareness ratio α is set to be 0.5. It is of interest for us that the local awareness ratio α has two-stage effects on the epidemic threshold β_c^U. The two-stage is divided at a fixed point $\alpha = 0.5$, with the first stage occurring in the range of $\alpha \in [0, 0.5)$ and the second stage happens when α belongs to [0.5,1]. In every stage, the change of α has little effect on the epidemic threshold. In order to explore if the critical point is related to the structure of multiplex network or the values of other parameters, including recovery probability μ and the probability of forgetting the awareness δ, we perform large amounts of simulations on different multiplex networks with different values of μ and δ.

In the following, we apply our LACS model to the case of two-layer Erdős-Rényi networks, of which the two layers are the same Erdős-Rényi networks. In FIG. 4, we examine the effect of local awareness ratio α on the change of epidemic threshold β_c^U.

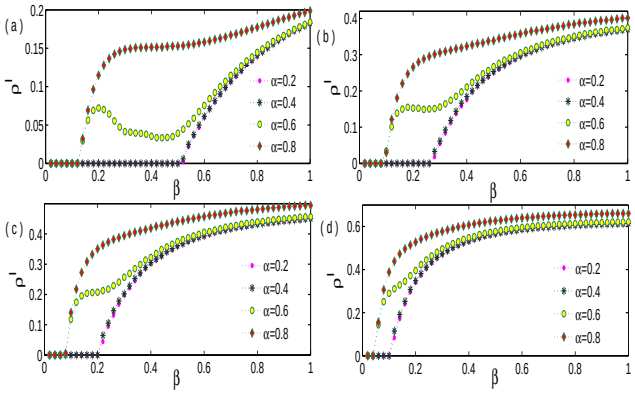

FIG. 4. (Color online)Monte Carlo simulations of two-layer Erdős-Rényi networks. The size of infected individuals ρ^I is shown as a function of infectivity β. In every panel, we plot this dynamic process on four different local awareness ratio α: $\alpha = 0.2$ (circle lower line), $\alpha = 0.4$ (cross line), $\alpha = 0.6$ (circle upper line), $\alpha = 0.8$ (diamond line). The values of the other two parameters are: (a) $\mu = 0.8, \delta = 0.3$, (b) $\mu = 0.6, \delta = 0.5$, (c) $\mu = 0.5, \delta = 0.6$, (d) $\mu = 0.3, \delta = 0.8$, respectively. The Erdős-Rényi network has 10^4 nodes and the average degree $\langle k\rangle$ is 5. All these simulations begin with the initial state where 10% of the nodes are infected and average 10 realizations for each curve on the same Erdős-Rényi networks.

Similar to SF networks, as can be seen from FIG. 4, in the case of Erdős-Rényi networks, it is found that the local awareness ratio also has the two-stage effects on epidemic threshold no matter what value δ and μ is. On this occasion, these simulations confirm that the two-stage effects appears invariably in our model, irrespectively of the value of δ and μ and the structure of networks as well. We have also explored other different structures of multiplex networks for the sake of completion, and in all of them, the two-stage effects exist. Besides, we have compared the UAU-SIS model[26] with LACS model(for more details, see Supplemental Material). All these simulations state one conclusion that the coupled dynamic process induces the appearance of two-stage effects on epidemic threshold. That is to say, this phenomenon suggests that the two-stage effects on epidemic threshold is a result of our LACS model with one layer being a threshold model and the other layer being a contagion model. In the next section, so as to explore this critical point, within the framework of LACS model, we use a 1D lattice model to analyze this phenomenon.

A. Analysis of the critical point on 1D lattice model

We consider a 1D lattice model in which each node has two neighbors with a total number of 10^4 nodes on each layer, see FIG. 5. As the degree of each node is 2, there exist only three cases of awareness states of its neighbors. The first case is none of them is aware of the epidemics, the second case is only one of them is aware of the epidemics, and the last one is both of them are aware of the epidemics. When $0 \leqslant \alpha < 0.5$, if none of the two neighbors is aware of the epidemics, the probability of an unaware node to be aware is 0, otherwise, the probability is 1; when $\alpha \geqslant 0.5$, if both of the two neighbors are aware of the epidemics, the probability of an unaware node to be aware is 1, otherwise, the probability is 0. In the following, we still use the MMCA method to study the epidemic threshold of the 1D lattice model. Furthermore, through the analysis, we illustrate the reason why two-stage effects on epidemic threshold occur at $\alpha = 0.5$.

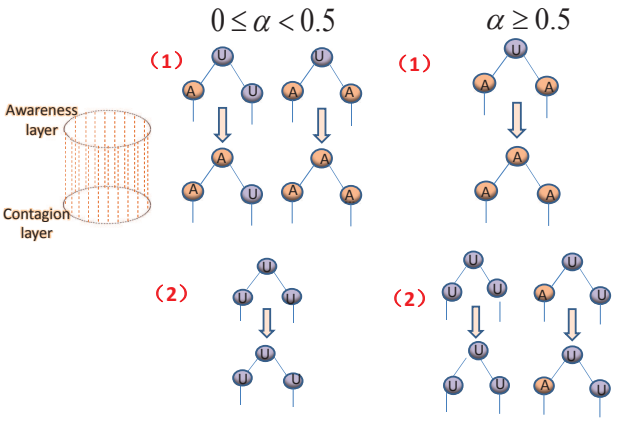

FIG. 5. Example of LACS model on 1D lattice model. In this figure, we describe the transitions of one unaware node under different local awareness ratios: when $0 \leqslant \alpha < 0.5$. (1) represents the two different cases where unaware node becomes aware.(2) represents the unique case where unaware node remains unaware; when $\alpha \geqslant 0.5$, (1) represents the unique case where unaware node becomes aware. (2) represents the two different cases where unaware node remains unaware.

To derive the epidemic threshold of the 1D lattice model, we recall that the fraction of unaware nodes is P_U, thus the fraction of aware nodes is $P_A = 1 - P_U$. Because of the homogeneity of lattice, we assume that the probability for one node being aware is P_A and the probability for one node being unaware is P_U. According to these definitions, let $P^{(j)}, j = 0, 1, 2$ be the probability that one node has i neighbors, of which the state is aware. Therefore, we have $P^{(0)} = P_U^2, P^{(1)} = 2P_U P_A, P^{(2)} = P_A^2$. Then, we obtain the probability tree of the lattice as FIG. 6.

Hence, through analyzing the states of the two neighbors of node i, using the MMCA method, we can get $P_i^{US}(t)$ and $P_i^{AS}(t)$ which represent the probabilities for node i being US state or AS state, respectively:

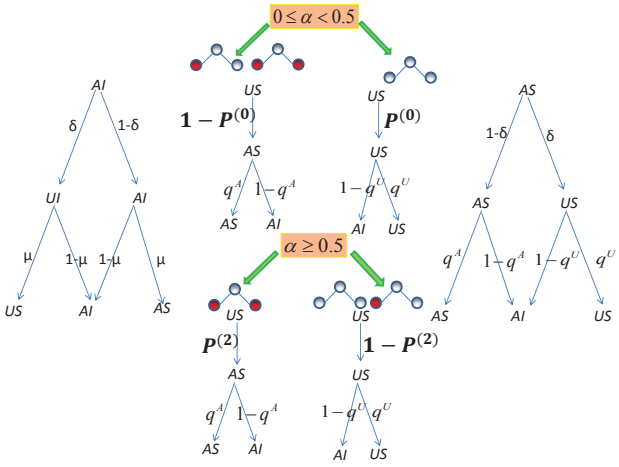

FIG. 6. Transition probability trees of 1D lattice model. The probability trees that AI and AS states transform into other states are the same with SF networks. As for the US state, because of the existence of critical awareness ratio $\alpha = 0.5$, there are two kinds of trees according to different local awareness ratios. In this figure, red node means that this node is aware and white means the node is unaware. $P^{(0)}$ is the probability that the awareness states of two neighbors are unaware, and $P^{(2)}$ is the probability that the awareness states of two neighbors are aware. The other parameters represent the same meanings as described in Sec. III

(1)$0 < \alpha < 0.5$

$$\begin{aligned} P_i^{US}(t+1) &= P_i^{AI}(t)\mu\delta + P_i^{AS}(t)\delta q_i^U + P_i^{US}(t)P^{(0)}q_i^U \\ P_i^{AS}(t+1) &= P_i^{AI}(t)\mu(1-\delta) + P_i^{AS}(t)(1-\delta)q_i^A \\ &+ P_i^{US}(t)(1-P^{(0)})q_i^A \end{aligned} \tag{10}$$

(2)$\alpha \geqslant 0.5$

$$\begin{aligned} P_i^{US}(t+1) &= P_i^{AI}(t)\mu\delta + P_i^{AS}(t)\delta q_i^U + P_i^{US}(t)(1-P^{(2)})q_i^U \\ P_i^{AS}(t+1) &= P_i^{AI}(t)\mu(1-\delta) + P_i^{AS}(t)(1-\delta)q_i^A \\ &+ P_i^{US}(t)P^{(2)}q_i^A \end{aligned} \tag{11}$$

Among Eqs.(10) and Eqs.(11), P_i^{AI} is the probability for node i being AI state and other parameters have the same meanings with our definitions of the LACS model in Sec.III. We use the same assumption as Eqs.(7) to derive stationary solution of Eqs.(10) and Eqs.(11). Thus, Eqs.(10) and Eqs.(11) can be described as follows:

(1)$0 < \alpha < 0.5$

$$\begin{aligned} P_i^{US} &= P_i^{AS}\delta + P_i^{US}P^{(0)} \\ P_i^{AS} &= P_i^{AS}(1-\delta) + P_i^{US}(1-P^{(0)}) \end{aligned} \tag{12}$$

(2)$\alpha \geqslant 0.5$

$$P_i^{US} = P_i^{AS}\delta + P_i^{US}(1 - P^{(2)})$$
$$P_i^{AS} = P_i^{AS}(1-\delta) + P_i^{US}P^{(2)} \quad (13)$$

Noting that $P^{(0)} = P_U^2, P^{(2)} = P_A^2$ and inserting them in Eqs.(12) and Eqs.(13) we obtain

(1)$0 < \alpha < 0.5$

$$P_i^{US} = P_i^{AS}\delta + P_U^2 P_i^{US} \approx P_i^{AS}\delta \quad (14)$$

Since we have $P_i^{US} + P_i^{AS} + P_i^{AI} = 1$ and $P_i^{AI} = \epsilon_i \ll 1$ around the epidemic threshold β_c, we can approximately get $P_i^{US} + P_i^{AS} = 1$. Therefore, it is clear for us that when $0 < \alpha < 0.5$, $P_i^{US} = \frac{1}{1+\frac{1}{\delta}}$.

(2)$\alpha \geqslant 0.5$

$$P_i^{US} = P_i^{AS}\delta + (1 - P^{(2)})P_i^{US} \approx P_i^{AS}\delta + P_i^{US} \quad (15)$$

which means that when $\alpha \geqslant 0.5$, $P_i^{AS} \approx 0$ and then $P_i^{US} \approx 1$. In FIG. 7, we show our analysis about the final size of unaware nodes around the epidemic threshold β_c.

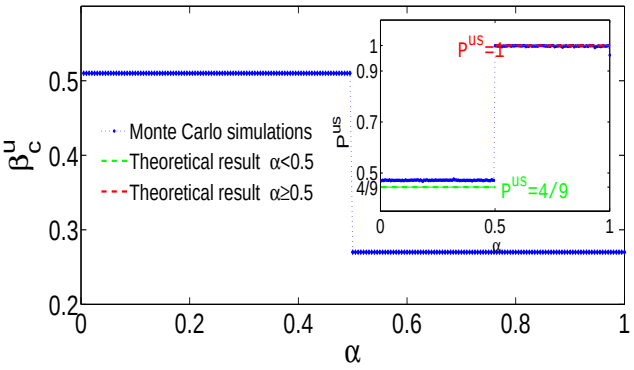

FIG. 7. (Color online)Plot of the epidemic threshold β_c^U as a function of local awareness ratio α. The two-stage effects on epidemic threshold occur at $\alpha = 0.5$, whereas the inset shows the comparison of theoretical analysis of $P^{US} = \frac{1}{N}\Sigma_i P_i^{US}$ (green and red dotted line) and the Monte Carlo simulations (blue dotted line) with $\delta = 0.8$. Note that when $\delta = 0.8$, our theoretical analysis of $P^{US} = \frac{1}{1+\frac{1}{\delta}} = \frac{4}{9}$ if $\alpha \in [0, 0.5)$, otherwise $P^{US} = 1$ on the 1D lattice model.

Eqs.(14) and (15) means that when $\alpha \in [0.5, 1]$, the final fraction of unaware nodes $P^{US} = \frac{1}{N}\sum_{i=1}^{N} P_i^{US} \approx 1$ around the epidemic threshold β_c, whereas when $\alpha \in [0, 0.5)$, $P^{US} \approx P^{AS}\delta \approx \frac{1}{1+\frac{1}{\delta}}$. These results lead to the two-stage effects on the epidemic threshold β_c^U for the reason that the more individuals know the epidemics, the bigger the epidemic threshold is. Therefore, as a result of different fractions of unaware individuals around 0.5, there exists an abrupt transition for the epidemic threshold. That is to say, the awareness cascade on upper layer leads to the two-stage effects of the epidemic threshold.

As to an epidemic, the epidemic threshold and the final epidemic size are two important characteristics to describe it. From the analysis above , we explore the two-stage effects of our LACS model on the epidemic threshold. Hence, in order to have a comprehensive understanding of the effects of LACS model on epidemics, in the following section, we study the effect of local awareness ratio on the final epidemic size.

B. The effect of local awareness ratio on the final epidemic size

In order to explore what effect the local awareness ratio has on the spreading of epidemics, we illustrate the spreading process in FIG. 8 and FIG. 9. In the two figures, we plot the stationary fraction of infected individuals ρ^I as a function of infectivity β^U and α using the SF multiplex networks defined in FIG. 3 with different values of recovery probability μ and the probability of forgetting the awareness δ.

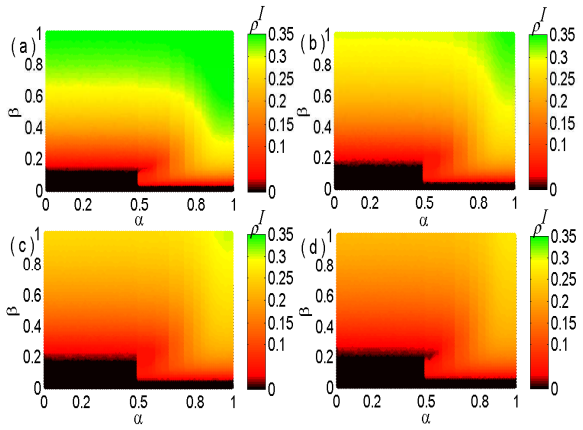

FIG. 8. (Color online)The stationary fraction of infected individual ρ^I as a function of infectivity β^U and the local awareness ratio α with the same value of $\delta = 0.4$ in every panel. Recovery probability μ is set as follows: (a) $\mu = 0.5$ (b) $\mu = 0.6$ (c) $\mu = 0.7$ (d) $\mu = 0.8$ from top left to bottom right. The four full phase diagrams $\beta - \alpha$ for the same multiplex network described in FIG. 3 are obtained by averaging 20 realizations for each point in the grid 100×100.

As can be seen from FIG. 8 and FIG. 9, it's clear that the effects α has on the spreading of epidemics can be classified into two categories, of which one is the final epidemic size ρ^I and the other is the epidemic threshold β_c^U. As for the final epidemic size, we find that local awareness ratio α plays two roles under different recovery probability μ and probability of forget the awareness δ. On the one hand, when $\alpha \in [0, 0.5)$, it has little effect on the final epidemic size; On the other hand, however, if $\alpha \in [0.5, 1]$, it has obvious effect on the final epidemic size, especially when α becomes larger and larger (also see Supplement Material). Furthermore, with a smaller δ and bigger μ, the final size of epidemic becomes smaller and smaller. It is obvious that the increasing of μ leads to a faster decreasing of final epidemic size than the decreasing of

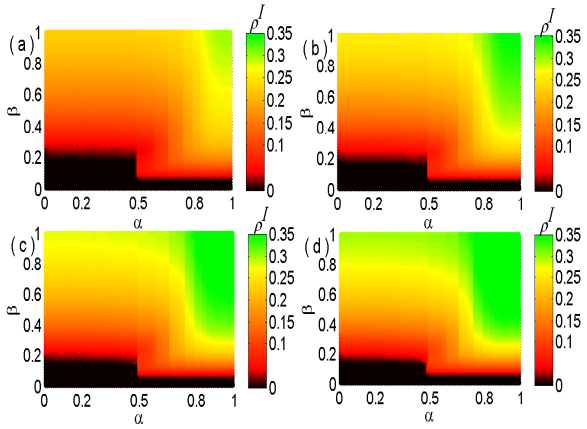

FIG. 9. (Color online)The stationary fraction of infected individual ρ^I as a function of infectivity β^U and the local awareness ratio α with the same value of $\mu = 0.9$ in every panel. The probability of forget the awareness δ is set as follows: (a) $\delta = 0.5$, (b) $\delta = 0.6$, (c)$\delta = 0.7$, (d) $\delta = 0.8$ from top left to bottom right. The four full phase diagrams $\beta - \alpha$ for the same multiplex network described in FIG. 3 are obtained by averaging 20 realizations for each point in the grid 100×100.

δ. This is because that μ is recovery probability which can directly effect the percentage of infected individuals, whereas δ is the probability of forgetting awareness which effects the percent of infected individuals through coupled dynamic process. At the same time, in all these cases, similar to FIG. 3 and FIG. 4, the epidemic threshold β_c^U has an abrupt transition at $\alpha = 0.5$, which has been discussed above on 1D lattice model.

Here let us go back to our LACS model to explore the reason of two-stage effects on final epidemic size. As α is the local awareness ratio, then if α becomes larger, the probability of unaware individuals to be aware becomes smaller. This can also lead the probability for individuals being infected become bigger for the reason that individuals can not take measures if they are unaware of the disease. But the bigger infectivity probability leads more individuals become aware, which can in turn promote the spreading of awareness. The coupled dynamic process determines the final epidemic size and it is balanced by the two factors' effects. Owing to the two-stage effects on the epidemic threshold, the epidemic threshold is grouped into two situations. When $\alpha < 0.5$, the effect of larger α on the promotion of epidemic spreading can be balanced by the effect of increasing popularity of awareness. However, when $\alpha \geq 0.5$, larger α shows a strong effect on promoting the spreading of epidemic and leads to larger fraction of infected individuals. Hence, the dynamic process of the two layers with different spreading models helps us understand the difference of final epidemic size when α is set to be various values.

V. CONCLUSIONS

In a summary, we have studied the effects of awareness spreading on the outbreak of epidemics in the framework of multiplex networks. Our results show that the local awareness ratio α has two-stage effects on epidemic threshold and leads to different final epidemic sizes, regardless of the structure of networks or the values of other parameters. That is to say, when α is in the range of [0,0.5), the epidemic threshold is a fixed and larger value, however, in the range of [0.5,1], the epidemic threshold is also a fixed but smaller value. As for the final epidemic size, it increases as the local awareness ratio α increases. But if $\alpha \in [0, 0.5)$, the increasing speed is much more slower than the speed when $\alpha \in [0.5, 1]$. These phenomena give us an interesting way to understand the epidemics in reality for they can somehow explain why some epidemics can not outbreak or reach the epidemic threshold. In reality, for some epidemics, if an individual is easy to take measures even though less than half of its friends know or are infected by some epidemics, which means that in our awareness spreading layer the local awareness ratio $\alpha < 0.5$. Since on the point the epidemic threshold is bigger, this leads to the outbreak failure of epidemics.

Furthermore, our results give us useful suggestions on the prevention of epidemics through different strategies. For some serious epidemics, the local awareness ratio α of an individual locates in [0,0.5) with large probability, which indicates that they don't need half of their neighbors to tell them the epidemics. Therefore, as the epidemic threshold is the bigger one and decreasing the local awareness threshold has little effect on the final epidemic size, what we should do is to try our best to separate and cure the infected individuals. But for some other epidemics, the bigger local awareness ratio α along with the smaller epidemic threshold sheds light on what measures we should take to lower the popularity of epidemics. We should broadcast epidemics through various social networks to catch individuals' attention and then decrease the local awareness ratio, which can not only make the final epidemic size become smaller but also increase the epidemic threshold. Finally, our LACS model can also be applied to various spreading processes, including rumor spreading, to have a better understanding of them.

VI. ACKNOWLEDGEMENT

We acknowledge anonymous referees for valuable comments and useful suggestions. This work is partially supported by the Chinese National Science Foundation under Grant No.11201017, No.11290141 and No.11401396, Cultivation Project of National Natural Science Foundation of China (91130019) and the International Cooperation Project of Ministry of Science and Technology of China (2010DFR00700). Q.G. also acknowledges financial support from China Scholarship Council. One of the

authors, J.X. is also supported by the DAAD scholarship for young scientist.

VII. SUPPLEMENTAL MATERIAL

In this section, we apply LACS model on various multiplex networks to explore the effects of local awareness ratio on the spreading of epidemics.

In FIG. 10, we explore the spreading process on two-layer Erdős-Rényi network, of which the two layers are the same Erdős-Rényi networks. Meanwhile, the Erdős-Rényi network has 10^4 nodes and the average degree $\langle k \rangle$ is 5.

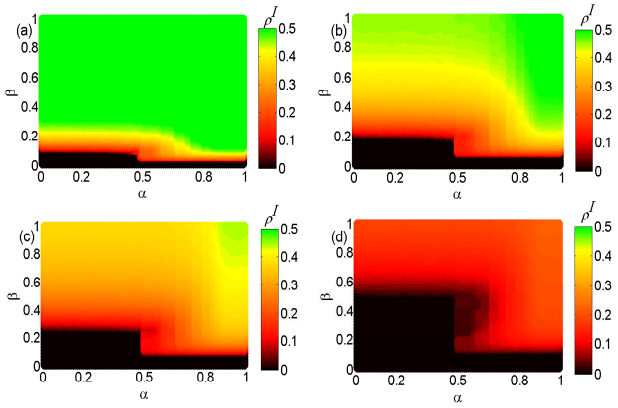

FIG. 10. (Color online)The stationary fraction of infected individual ρ^I as a function of infectivity β^U and the local awareness ratio α. The parameters are set as follows: (a) $\mu = 0.3, \delta = 0.8$, (b) $\mu = 0.5, \delta = 0.6$, (c)$\mu = 0.6, \delta = 0.5$, (d) $\mu = 0.8, \delta = 0.3$ from top left to bottom right. The four full phase diagrams $\beta - \alpha$ are obtained by averaging 20 Monte Carlo simulations for each point in the grid 100×100. All these simulations begin with the initial state where 10% of the nodes are infected on the two-layer Erdős-Rényi networks.

In FIG. 11, we also explore the spreading process on one multiplex network with two different layers. The awareness layer is Erdős-Rényi network defined above and the contagion layer is SF network which consists of 10^4 nodes generated by the configuration model with exponent 3. Besides, the average degree of the SF network is 6.

It is clear that the two-stage effects also exist in these multiplex networks, no matter what kinds of networks the two layers belong to. It is also interesting that increasing β in a certain range, the awareness cascade overcomes the infection cascade when $\mu \gg \delta$, such as, FIG. 8(d), FIG. 10(d), FIG. 11(d). In addition, as can be seen from these figures, the overcome phenomenon is especially remarkable on the two-layer Erdős-Rényi multiplex network. Hence, in order to explore the reason why there exists this interesting phenomenon, let's consider the details of the coupled spreading process. As described in the main text, μ is the probability of recovering from

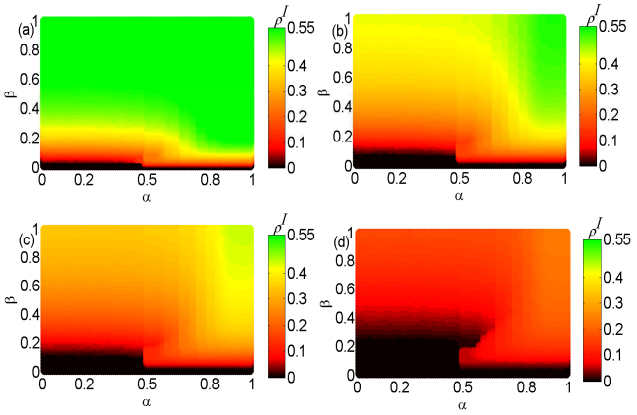

FIG. 11. (Color online)The stationary fraction of infected individual ρ^I as a function of infectivity β^U and the local awareness ratio α. The parameters are set as follows: (a) $\mu = 0.3, \delta = 0.8$, (b) $\mu = 0.5, \delta = 0.6$, (c)$\mu = 0.6, \delta = 0.5$, (d) $\mu = 0.8, \delta = 0.3$ from top left to bottom right. The four full phase diagrams $\beta - \alpha$ are obtained by averaging 20 Monte Carlo simulations for each point in the grid 100×100. All these simulations begin with the initial state where 10% of the nodes are infected on the multiplex network with two different layers.

epidemics for infected node and δ is the probability of being unaware for aware node, respectively. Therefore, with the increasing of β, more and more nodes become infected, at the same time, larger μ leads more nodes become susceptible and smaller δ makes more nodes stay aware. This coupled dynamic process produces more and more nodes whose states are AS, which can slow down the speed of spreading process. If the promotion effect of lager β is not so strong to overcome the effect of μ and δ, the fraction of infected nodes ρ^I becomes smaller instead of increasing with β. With respect to the difference between Erdős-Rényi multiplex network and SF multiplex network, it is important to compare the different structures of these two kinds of network. Because of the preferential attachment, SF network has a more widely degree distribution than ER network. According to our LACS model, it is somehow difficult for unaware hub nodes being aware on SF network, which means that larger μ and smaller δ produces more US nodes instead of AS nodes. Since the AS nodes can not only decrease ρ^I but also promote the spreading of awareness, the slowing down effect on the spreading process of SF network is not so strong as Erdős-Rényi network. This can also be seen through comparing FIG. 8(d), which is a two-layer SF network, with FIG. 11(d), of which the awareness layer is Erdős-Rényi network and the other is SF network. Although the difference between these two multiplex networks is just the structure of awareness layer, the overcome phenomenon of SF multiplex network is much less obvious than the one including one Erdős-Rényi layer. Therefore, the phenomenon also indicates the importance of awareness spreading on the coupled dynamic process.

In the following, we also compare the UAU-SIS model [26] with LACS model on a two-layer SF multiplex network as defined in FIG. 3. Since unaware nodes in the UAU-SIS model can become aware with a probability λ through communication with their neighbors, which is different with threshold model, we have compared these two models on different conditions of λ and local awareness ratio α, as can be seen from FIG. 12, FIG. 13.

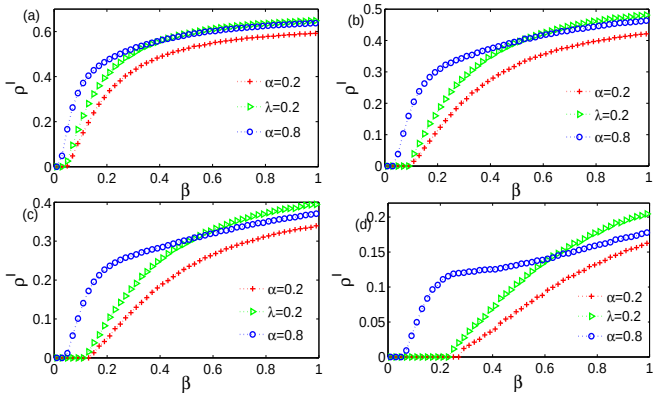

FIG. 12. (Color online.) Monte Carlo simulations of LACS model (blue circle and red plus sign lines) and the UAU-SIS model (green triangle line), the initial fraction of infected nodes is set to be 10%. In the four panels, we plot the stationary fraction of infected individual ρ^I as a function of infectivity β^U for a fixed value of $\lambda = 0.2, \alpha = 0.2, \alpha = 0.8$. The other parameters are set as follows: (a) $\mu = 0.3, \delta = 0.8$ (b) $\mu = 0.5, \delta = 0.6$ (c) $\mu = 0.6, \delta = 0.5$ (d) $\mu = 0.8, \delta = 0.3$, respectively.

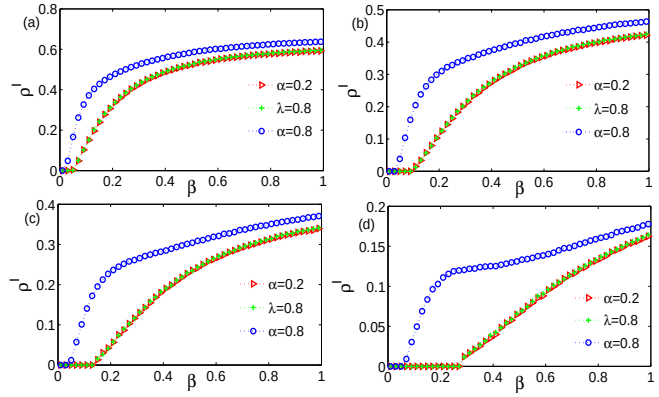

FIG. 13. (Color online.) Monte Carlo simulations of LACS model (blue circle and red triangle lines) and the UAU-SIS model (green plus sign line), the initial fraction of infected nodes is set to be 10%. In the four panels, we plot the stationary fraction of infected individual ρ^I as a function of infectivity β^U for a fixed value of $\lambda = 0.8, \alpha = 0.2, \alpha = 0.8$. The other parameters are set as follows: (a) $\mu = 0.3, \delta = 0.8$ (b) $\mu = 0.5, \delta = 0.6$ (c) $\mu = 0.6, \delta = 0.5$ (d) $\mu = 0.8, \delta = 0.3$, respectively.

As shown in FIG. 12 and FIG. 13, the dynamic processes of these two models are different from each other

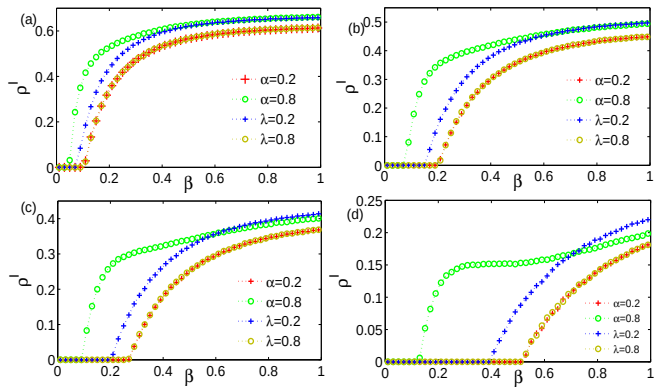

FIG. 14. (Color online.) Monte Carlo simulations of LACS model (green circle (upper) and red plus sign (lower) lines) and the UAU-SIS model (yellow circle (lower) and blue plus sign (upper) line) on two-layer ER network defined in FIG. 4, the initial fraction of infected nodes is set to be 10%. In the four panels, we plot the stationary fraction of infected individual ρ^I as a function of infectivity β^U for a fixed value of $\lambda = 0.2, \lambda = 0.8, \alpha = 0.2, \alpha = 0.8$. The other parameters are set as follows: (a) $\mu = 0.3, \delta = 0.8$ (b) $\mu = 0.5, \delta = 0.6$ (c) $\mu = 0.6, \delta = 0.5$ (d) $\mu = 0.8, \delta = 0.3$, respectively.

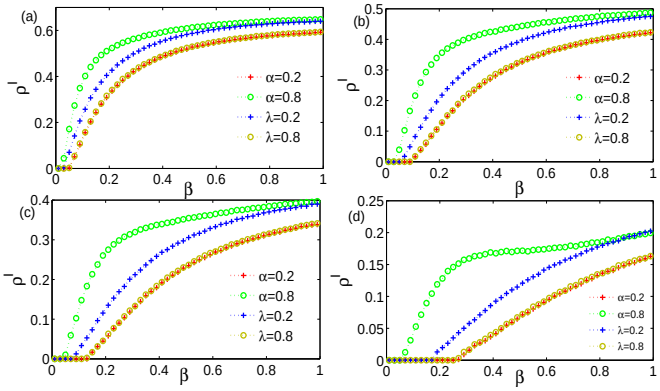

FIG. 15. (Color online.) Monte Carlo simulations of LACS model (green circle (upper) and red plus sign (lower) lines) and the UAU-SIS model (yellow circle (lower) and blue plus sign (upper) line) on one multiplex network defined in FIG. 11, of which the awareness layer is ER network and the other layer is SF network. The initial fraction of infected nodes is set to be 10%. In the four panels, we plot the stationary fraction of infected individual ρ^I as a function of infectivity β^U for a fixed value of $\lambda = 0.2, \lambda = 0.8, \alpha = 0.2, \alpha = 0.8$. The other parameters are set as follows: (a) $\mu = 0.3, \delta = 0.8$ (b) $\mu = 0.5, \delta = 0.6$ (c) $\mu = 0.6, \delta = 0.5$ (d) $\mu = 0.8, \delta = 0.3$, respectively.

according to the value of λ: When $\lambda \ll 1$, the epidemic threshold of the UAU-SIS model β_c^{UAU} satisfies $\beta_c^{\alpha 1} \leqslant \beta_c^{UAU} < \beta_c^{\alpha 2}$, where $\beta_c^{\alpha 1}, \beta_c^{\alpha 2}$ represents the small and large epidemic threshold of LACS model, respectively. Therefore, through considering the awareness layer as a threshold model, abundant details about the outbreak of epidemics have been obtained. Besides, with

the increasing of β, final epidemic size of the UAU-SIS model increases quickly than LACS model whatever α is. However, when $\lambda \to 1$, the dynamic process of the UAU-SIS model is almost the same with that of LACS model with small α. Noting that the difference between these two models is the definition of the probability of unaware node being aware. Thus, when $\lambda \to 1$, this means that the probability of unaware node i being aware is almost 1 if node i has aware neighbors. At the same time, since when α is smaller than 0.5, the spreading process on LACS model is almost the same, for simplicity, we consider an critical point that $\alpha \to 0$. It is obvious that when $\alpha \to 0$, the probability for unaware node i being aware is also almost 1 if node i has aware neighbors. This induces that the dynamic processes on these two models are almost the same.

In order to verify our analysis, we have also compared the UAU-SIS model with LACS model on different multiplex networks in FIG. 14, FIG. 15. The results show that when $\lambda \to 1$ and α is smaller than 0.5, the dynamic processes of the two models are always almost the same no matter what structure the multiplex network is. Therefore, through the comparison between the UAU-SIS model with LACS model, we have also cross-checked LACS model. From the analysis above, we find that the LACS model gives us a better understanding of the UAU-SIS model and reveals abundant details of epidemic spreading.

[1] R. Pastor-Satorras and A. Vespignani, Phys. Rev. Lett. 86, 3200 (2001).
[2] M. E. J. Newman, Phys. Rev. E 66, 016128 (2002).
[3] R. Pastor-Satorras and A. Vespignani, Phys. Rev. E 63, 066117 (2001).
[4] R. M. May and A. L. Lloyd, Phys. Rev. E 64, 066112 (2001).
[5] Y. Moreno, R. Pastor-Satorras and A. Vespignani, Eur. Phys. J. B 26, 521 (2002)
[6] Z. Dezso and A.-L. Barabási, Phys. Rev. E 65, 055103 (2002).
[7] M. Boguná and R. Pastor-Satorras, Phys. Rev. E 66, 047104 (2002).
[8] T. Gross, C. J. D. D'Lima and B. Blasius, Phys. Rev. Lett.96, 208701 (2006).
[9] D. Balcan, A. Vespignani, Nat. Phys. 7, 581 (2011).
[10] S. Meloni, N. Perra, A. Arenas, S. Gómez, Y. Moreno, and A. Vespignani, Sci. Rep. 1, 62 (2011).
[11] N. T. J. Bailey, The Mathematical Theory of Infectious Diseases, Springer, 1975.
[12] A. Grabowski, R.A. Kosiński, Phys. Rev. E 70, 031908 (2004).
[13] M. J. Keeling, and K. T. D. Eames, J. R. Soc. Interface 2, 295 (2005).
[14] S. Funk, M. Salathé, and V. A. Jansen, J. R. Soc. Interface 7, 1247 (2010).
[15] E. Cozzo, R. A. Banos, S. Meloni, Y. Moreno, Phys. Rev. E 88, 050801 (2013).
[16] M. Salathé, M. Kazandjieva, J. W. Lee, P. Levis, M. W. Feldman, and J. H. Jones, Proc. Natl. Acad. Sci. U. S. A. 107, 22020 (2010).
[17] R. R. Kao, M. B. Gravenor, M. Baylis, C. J. Bostock, C. M. Chihota, J. C. Evans, W. Goldmann, A. J. A. Smith, A. R. McLean, Science 295, 332(2002).
[18] V. E. Vergu, H. Busson, and P. Ezanno, PloS one 5, e9371 (2010).
[19] G. Hartvigsena, J. M. Dresch, A. L. Zielinski, A. J. Macula, C. C. Leary, J. Theor. Biol. 246, 205 (2007).
[20] N. Perra, D. Balcan, B. Goncalves, and A. Vespignani, PloS one 6, e23084 (2011).
[21] N. Perra, B. Goncalves, R. Pastor-Satorras, and A. Vespignani, Sci. Rep. 2, 469 (2012).
[22] Z. Wang, H. Zhang, Z. Wang, Chaos 61, 1 (2014).
[23] C. Granell, S. Gómez, and A. Arenas, Phys. Rev. E 90, 012808 (2014).
[24] S. Funk, E. Gilad, C. Watkins, and V. A. A. Jansen, Proc. Natl. Acad. Sci. U. S. A. 106, 6872 (2009).
[25] Q. Wu, X. Fu, M. Small, and X.-J. Xu, Chaos 22, 013101 (2012).
[26] C. Granell, S. Gómez, and A. Arenas, Phys. Rev. Lett. 111, 128701(2013).
[27] P. J. Mucha, T. Richardson, K. Macon, M. A. Porter, and J.-P. Onnela, Science 328, 876 (2010).
[28] M. Szell, R. Lambiotte, and S. Thurner, Proc. Natl. Acad. Sci. U. S. A. 107, 13636 (2010).
[29] E. Cozzo, A. Arenas, Y. Moreno, Phys. Rev. E 86, 036115 (2012).
[30] S. Gómez, A. Diaz-Guilera, J. Gómez-Gardeñes, C. J. Pérez-Vicente, Y. Moreno, and A. Arenas, Phys. Rev. Lett. 110, 028701 (2013).
[31] S. Boccaletti, G. Bianconi, R. Criado, C.I. del Genio, J. Gómez-Gardeñes, M. Romance, I.Sendiña-Nadal, Z. Wang, M. Zanin, Phys. Rep. in press. (2014)
[32] Z. Wang, L. Wang, M. Perc, Phys. Rev. E 89, 052813 (2014).
[33] D. J. Watts, Proc. Natl. Acad. Sci. U. S. A. 99, 5766 (2002).
[34] S. Melnik, J. A. Ward, J. P. Gleeson, and M. A. Porter, Chaos 23, 013124 (2013).
[35] J. Borge-Holthoefer, R. A. Baños, S. González-Bailón, and Y. Moreno, J. Complex Networks 1, 3 (2013).
[36] D. Chakrabarti, Y. Wang, C. Wang, J. Leskovec, and C. Faloutsos, ACM Trans. Inf. Syst. Secur. 10, 1 (2008).
[37] S. Gómez, A. Arenas, J. Borge-Holthoefer, S. Meloni, and Y. Moreno, Europhys. Lett. 89, 38009 (2010).